

Local wave field synthesis of a moving point source using temporal bandlimitation

Gergely Firtha¹, Nara Hahn², Frank Schultz³, Péter Fiala¹

¹ *Dept. of Networked Systems and Services, Budapest University of Technology and Economics, Email: firtha/fiala@hit.bme.hu*

² *Institute of Sound and Vibration Research, University of Southampton, Email: nara.hahn@soton.ac.uk*

³ *Institute of Communications Engineering, University of Rostock, Email: frank.schultz@uni-rostock.de*

Introduction

The aim of sound field synthesis is to reproduce a virtual target sound field over an extended listening area using a densely spaced loudspeaker arrangement, usually termed as the secondary source distribution (SSD). By feeding the loudspeakers with specific driving functions, the superposition of sound fields from each SSD element should ideally match the target sound field in the intended receiving area. One prominent sound field synthesis method is Wave Field Synthesis (WFS) [1, 2].

As WFS obtains the necessary driving functions from a suitable boundary integral representation of the target sound field, perfect phase correct field-reconstruction could be only achieved by employing a theoretical, continuous secondary source distribution. In practical scenarios, however, the SSD consists discrete loudspeaker elements, leading to the emergence of secondary wavefronts, known as aliasing waves, alongside the intended virtual wavefront, severely degrading reproduction quality [3, 4].

Recently, a novel antialiasing strategy has been proposed by the present authors, achieving the suppression of the aliasing wavefronts by simple temporal bandlimitation of the loudspeaker feeds [5, 6]. However, this approach introduces artifacts stemming from the band limitation of the synthesized field to an upper frequency limit (determined by the direction of the virtual wavefront) consequently leading to noticeable coloration in the synthesis. To tackle this challenge, the current study presents a solution by enabling full-band synthesis through the introduction of a suitable filter design strategy beyond the aliasing frequency.

Theoretical basics

Local propagation vector: Consider an arbitrary steady-state sound field at an angular frequency ω . As a standard ansatz in the field of geometrical acoustics the sound field at a spatial position $\mathbf{x} = [x y z]^T$ is written in the general polar form as

$$P(\mathbf{x}, \omega) = A^P(\mathbf{x}) e^{-j \frac{\omega}{c} \phi^P(\mathbf{x})}, \quad (1)$$

where $A^P(\mathbf{x}, \omega)$ and $\phi^P(\mathbf{x})$ are real-valued functions, and c denotes the speed of sound. This formulation applies to both plane waves and (3D) point sources. The propagation characteristics of the sound field are governed by its phase function $\phi^P(\mathbf{x})$, which defines the local propagation vector $\hat{\mathbf{k}}^P(\mathbf{x})$:

$$\hat{\mathbf{k}}^P(\mathbf{x}) = [\hat{k}_x^P(\mathbf{x}), \hat{k}_y^P(\mathbf{x}), \hat{k}_z^P(\mathbf{x})]^T = \nabla_{\mathbf{x}} \phi^P(\mathbf{x}, \omega). \quad (2)$$

The local propagation vector is a unit vector perpendicular to the wavefront, pointing in the direction of local propagation [7].

2.5D Wave Field Synthesis: Consider a smooth, closed and convex secondary source distribution (SSD) contour, located at $\mathbf{x}_0 = [x_0, y_0, 0]^T$ consisting of a continuous distribution of 3D point sources, described by the 3D Green's function. Under high-frequency assumptions, the synthesized field inside the SSD at a receiver position $\mathbf{x} = [x, y, 0]^T$ can be described by the Kirchhoff approximation of 2.5D Kirchhoff-Helmholtz integral. From this integral representation the 2.5D driving functions can be extracted as [7]

$$D(\mathbf{x}_0, \omega) = \sqrt{8\pi} \underbrace{\sqrt{\frac{j\omega}{c}}}_{H_{\text{pre}}(\omega)} w(\mathbf{x}_0) \sqrt{d_{\text{ref}}(\mathbf{x}_0)} \hat{k}_n^P(\mathbf{x}_0) P(\mathbf{x}_0, \omega) \quad (3)$$

where $k_n^P(\mathbf{x}_0)$ is the normal component of the local wavenumber vector. The driving function consists of a pre-equalization filter $H_{\text{pre}}(\omega)$ [2, 1, 8], a secondary source selection window $w(\mathbf{x}_0)$ [9], a gain factor $\sqrt{d_{\text{ref}}(\mathbf{x}_0)}$ allowing amplitude correction along a reference curve, depending on the actual virtual field model (cf. [2, 7]) and the virtual field measured on the SSD.

The pre-equalization filter holds particular significance in the context of the current study. Functioning as a half-differentiator, it addresses the frequency response of a continuous linear point-source distribution, guaranteeing a flat SSD response.

Aliasing artifacts in WFS The backbone of WFS theory assumes a continuous secondary source distribution. In practical scenarios, the SSD consists of regularly spaced discrete source elements. Consequently, the individual secondary sources generate aliasing wavefronts superimposed to the desired virtual wavefront, giving rise to spatial aliasing phenomena. Although localization does not degrade due to the precedence effect, aliasing is perceived as strong coloration in the high-frequency region varying with the receiver position and the virtual source position/direction.

WFS with temporal antialiasing filtering

In order to avoid aliasing a straightforward strategy would be spatially bandlimiting the driving functions to the sampling wavenumber prior to SSD discretization. However, implementing this strategy necessitates analytical spatial filtering. Moreover, it proves impractical for

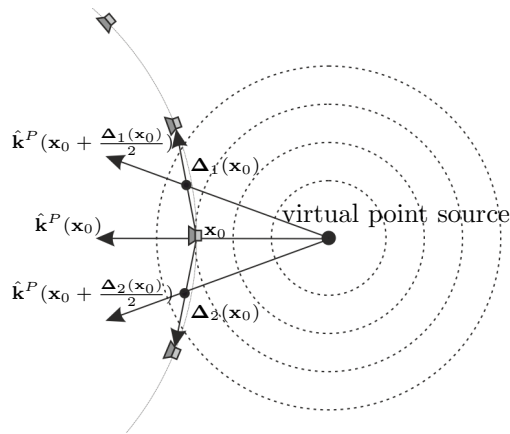


Figure 1: Geometry for defining the local aliasing frequency.

non-uniformly sampled SSD setups, commonly encountered in 3D Wave Field Synthesis (WFS) applications. Previous research by the current authors demonstrated that, due to the inherent temporal-spatial interconnection within the driving functions (stemming from wave propagation properties), spatial filtering can be viewed as an equivalent temporal filtering process. As a result, by bandlimiting the driving functions to the corresponding local aliasing frequency

$$\omega_c(\mathbf{x}_0) = c \frac{\pi}{\hat{k}_t^P(\mathbf{x}_0) \Delta x} \quad (4)$$

aliasing wavefronts can be efficiently suppressed. Here, Δx denotes the sampling distance (corresponding to the sampling arc length for curved SSD geometries), while $\hat{k}_t^P(\mathbf{x}_0)$ represents the tangential component of the local propagation vector.

This approach is valid for locally planar SSD and virtual wavefront configurations. However, it becomes invalid when dealing with a virtual point source near the SSD or a curved SSD with a relatively large sampling distance compared to its radius. To address these limitations, a straightforward workaround is proposed to accommodate the curvature of both the virtual wavefront and the SSD.

Inclusion of SSD and virtual wavefront curvatures

To obtain a more reliable approximation of the local aliasing frequency it is important to recognize that in equation (4) $\hat{k}_t^P(\mathbf{x}_0) \Delta x$ represents the sampling distance along the tangential direction of the local propagation vector.

To account for the SSD curvature we define the local sampling vector, comprising two vectors in the present 2.5D scenario, pointing from each SSD position to the adjacent SSD elements, thereby assuming a piecewise linear SSD. In Figure 1, these local sampling vectors are labeled as $\Delta_i(\mathbf{x}_0)$. In this geometry the sampling distance into the direction of the local propagation vector is obtained as the projection of these sampling vectors to the local propagation vectors given by $\langle \Delta_i(\mathbf{x}_0) \cdot \hat{\mathbf{k}}^P(\mathbf{x}_0) \rangle$. Obviously, the local aliasing frequency of the SSD element is

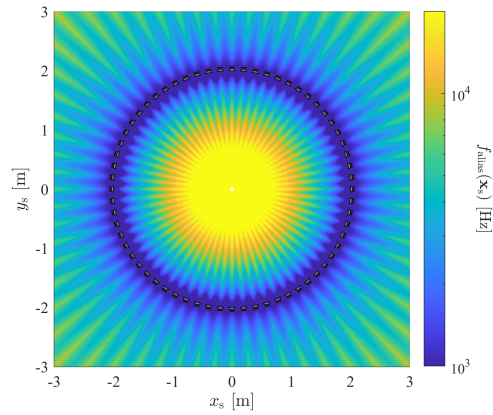


Figure 2: Maximal aliasing frequency as the function of the virtual source position.

defined by the maximum of the above directional sampling distances.

Moreover, if the virtual source is close to the SSD, its local propagation vector's direction varies significantly even between two adjacent SSD samples. To accommodate this directional change, as a conservative estimate, the local propagation vector is assessed between the SSD elements, specifically at $\mathbf{x}_0 + \frac{\Delta_i(\mathbf{x}_0)}{2}$. Taking all these factors into account, the local aliasing frequency is approximated as follows:

$$\omega_{\text{alias}}(\mathbf{x}_0) = c \frac{\pi}{\max_i \left\langle \Delta_i(\mathbf{x}_0) \cdot \hat{\mathbf{k}}^P\left(\mathbf{x}_0 + \frac{\Delta_i(\mathbf{x}_0)}{2}\right) \right\rangle}.$$

Having found a suitable approximation for the local aliasing frequency, antialiasing filtering can be performed by bandlimiting each SSD element to its aliasing frequency. The antialiasing strategy is discussed in details in [6].

Full-bandwidth antialiasing filter design A primary limitation of the above antialiasing strategy is that the synthesized field is bandlimited to the maximum aliasing frequency, which, in the case of a curved SSD, remains finite even when dealing with a virtual plane wave. The maximal aliasing frequency, and consequently, the synthesized field's bandwidth, diminishes notably as a virtual point source moves closer to the SSD. Consequently, the overall synthesis bandwidth heavily relies on the virtual source's position, leading to a noticeable deterioration in synthesis quality. The synthesized field's bandwidth, depicted in Figure 2 as a function of the virtual source's position, in case of a circular SSD with the radius of 2 m and consisting of 64 SSD elements.

To address this constraint, the following modification of the antialiasing strategy is proposed: Above the maximal aliasing frequency, one stationary SSD element, or two near-stationary elements, are selected. "Stationary" implies that the normal of the SSD element aligns with the local propagation direction of the virtual wave. "Near-stationary" refers to the two SSD elements between which the virtual source lies, denoted by \mathbf{x}_0^i in

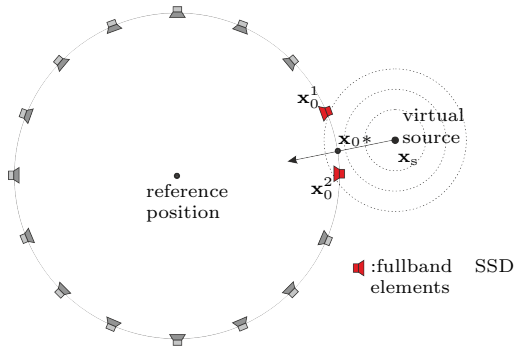


Figure 3: Geometry depicting the fullband SSD elements.

Figure 3. These SSD elements are designated as fullbandwidth, meaning no anti-aliasing filtering is applied to them. However, above their local aliasing frequency, several factors need to be considered to ensure a flat frequency response and accurate localization:

- Above the maximal aliasing frequency, only the stationary/near-stationary SSD elements are active. Consequently, the WFS prefilters, which typically compensate for the frequency response of a contour of secondary sources, yield an overall frequency response of $\sqrt{j\omega}$. This phenomenon requires compensation via a suitable inverse filter, represented as $\frac{1}{\sqrt{1+j\frac{\omega}{\omega_{\text{alias}}(\mathbf{x}_0)}}}$.
- If the virtual source is positioned between two near-stationary SSD elements, rather than a continuous wavefront, the field of two individual point sources is received at the reference position. Therefore, to maintain the amplitude and phase of the virtual wavefront, the energy of the active sources must be preserved at unity. Additionally, the phase of the two active sources should match the phase of the virtual wavefront on the SSD contour (denoted by \mathbf{x}_0^* in Figure 3). Energy preservation can be achieved by applying normalized Vector Base Amplitude Panning (VBAP) gains to the WFS driving functions above the aliasing frequency (g_i), while identical phase is ensured by applying phase shifts $\Delta\tau_i$ to the active secondary sources.

With the above considerations the antialiasing filter bank for the entire SSD is given by

$$H_{\text{aa}}(\mathbf{x}_0) = \frac{1}{\sqrt{1 + \left(\frac{\omega}{\omega_{\text{alias}}(\mathbf{x}_0)}\right)^{2N}}}, \quad (5)$$

while for the stationary/near-stationary SSD elements the antialiasing filters read as

$$H_{\text{aa}}(\mathbf{x}_0^i) = \frac{H_{\text{aa}}(\mathbf{x}_0^i) + g_i e^{j\omega\Delta\tau_i} (1 - H_{\text{aa}}(\mathbf{x}_0^i))}{\sqrt{1 + \frac{j\omega}{\omega_{\text{alias}}(\mathbf{x}_0^i)}}}. \quad (6)$$

The resulting filter bank is depicted in Figure 4 in case the virtual point source is located between two SSD elements, i.e. two near-stationary SSD elements exist.

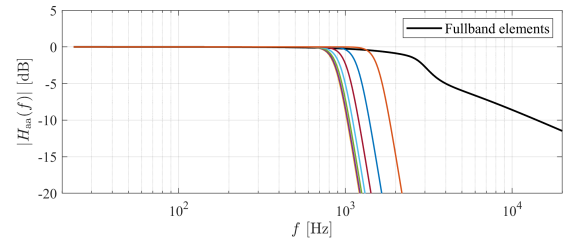


Figure 4: Antialiasing filter bank.

Results The result of the above fullband antialiasing strategy is depicted in Figure 5 in case of a virtual point source, located 2.9 m far from the origin (reference position).

In case of Figure 5 (a) the source is aligned with an SSD element, i.e. a stationary SSD element exists, being the single active secondary source above the maximal aliasing frequency. In case of Figure 5 (b) the source is between two SSD elements, i.e. two near-stationary SSD elements are active above the aliasing frequency.

The maximal aliasing frequency is denoted by dashed red line. It is important to recognize that this frequency constitutes a frequency limit above which no wavefront synthesis is achieved.

The figures verify that under this frequency limit aliasing artifacts are significantly suppressed. Deviations from the ideal flat frequency response of the virtual sound source remain below 3 dB, i.e. can be considered unperceivable. Above the aliasing frequency amplitude and direction correct synthesis is achieved in a sense that the local propagation is correctly reproduced in the reference position, inherently ensured by applying VBAP gains.

Finally, Figure 6 depicts the mean fullband error of synthesis at the reference position as the function of virtual source position, defined as

$$E_{\text{mean}}(\mathbf{x}_s) = \frac{1}{N_f} \sum_f \left| 20 \log_{10} \left| \frac{P_{\text{synth}}(f, \mathbf{x} = 0, \mathbf{x}_s)}{P_{\text{synth,ref}}(f, \mathbf{x} = 0, \mathbf{x}_s)} \right| \right|. \quad (7)$$

The reference field $P_{\text{synth,ref}}$ is given by the synthesized field using a quasi-continuous SSD, consisting of 1024 elements. Again, it is verified that the error resulting from the discretization of the SSD remains below the threshold of human hearing except for virtual sources in the immediate proximity of the SSD.

Conclusion

The present contribution discussed an antialiasing strategy for WFS, relying merely on the temporal bandlimitation of the driving functions. It was shown that bandlimiting each SSD element to its local aliasing frequency ensures a nearly aliasing free synthesis. A simple geometrical approach was introduced for the correct estimation of the local aliasing frequencies, with accounting for the curvature of the SSD and the virtual wavefront. In order to avoid the overall bandlimitation of the synthesis, full-band SSD elements are assigned, for which unique antialiasing filters are applied, ensuring amplitude, phase

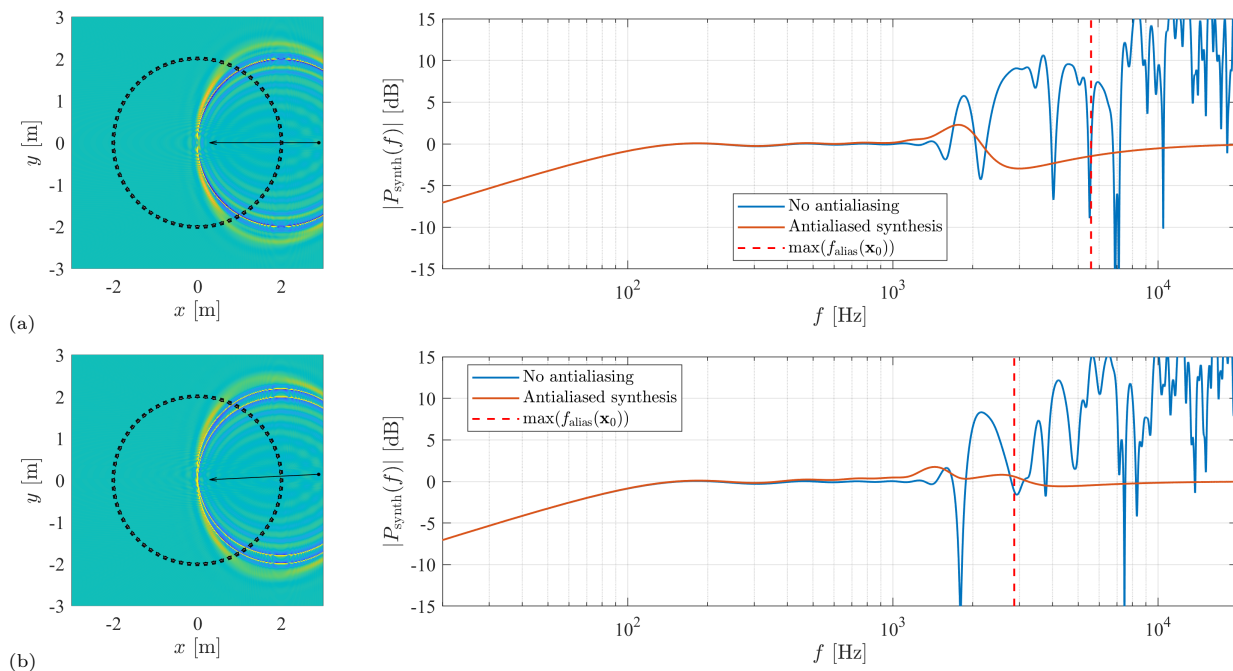


Figure 5: Result of synthesis applying the introduced antialiasing filtering strategy.

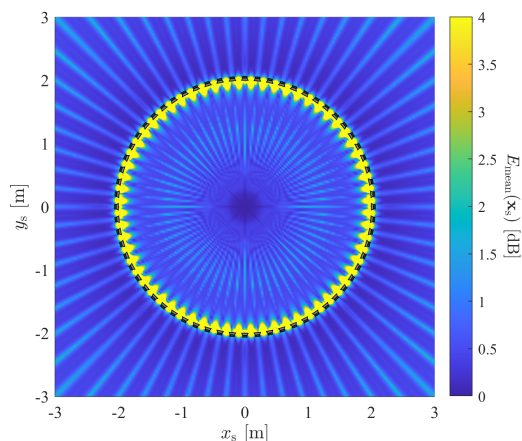


Figure 6: Mean error of synthesis as the function of the virtual source position.

and directionally correct synthesis even above the maximal aliasing frequency. The extension of the present approach towards arbitrary reference position (i.e. performing LWFS) is the topic of further research.

Acknowledgement

This work was supported by the János Bolyai Research Scholarship of the Hungarian Academy of Science, by the ÚNKP-23-5-BME-465 New National Excellence Program of the Ministry for Innovation and Technology from the source of the National Research, Development and Innovation Fund and by the OTKA PD-143129 and OTKA K-143436 grants.

References

[1] A.J. Berkhout, D. de Vries, and P. Vogel. Acoustic control by wave field synthesis. *J. Acoust. Soc. Am.*, 93(5):2764–2778, 1993.

- [2] E.W. Start. *Direct sound enhancement by wave field synthesis*. PhD thesis, Delft University of Technology, 1997.
- [3] F. Winter, H. Wierstorf, C. Hold, F. Krüger, A. Raake, and S. Spors. Colouration in local wave field synthesis. *IEEE/ACM Transactions on Audio, Speech, and Language Processing*, 26(10):1913–1924, October 2018.
- [4] F. Winter, F. Schultz, G. Firtha, and S. Spors. A geometric model for prediction of spatial aliasing in 2.5d sound field synthesis. *IEEE/ACM Transactions on Audio, Speech, and Language Processing*, 27(6):1031–1046, June 2019.
- [5] G. Firtha and P. Fiala. An analytic method for transforming spatial filtering of wfs driving functions into temporal filtering. In *DAGA2023*, Hamburg, March 2023.
- [6] Gergely Firtha, Nara Hahn, Frank Schultz, and Péter Fiala. Local wave field synthesis by temporal bandlimitation. In *2023 Immersive and 3D Audio: from Architecture to Automotive (I3DA)*, pages 1–10, 2023.
- [7] G. Firtha, P. Fiala, F. Schultz, and S. Spors. Improved referencing schemes for 2.5d wave field synthesis driving functions. *IEEE/ACM Trans. Audio, Speech, Lang. Process.*, 25(5):1117–1127, May 2017.
- [8] N. Bleistein. Two-and-one-half dimensional in-plane wave propagation. *Geophysical Prospecting*, pages 686–703, August 1986.
- [9] S. Spors. Extension of an analytic secondary source selection criterion for wave field synthesis. In *Proc. of the 123rd Audio Eng. Soc. Convention*, New York, October 2007.